

A cyclohexane-1,2-diyl-dinitrilotetraacetate tetrahydroxamate derivative for actinide complexation: synthesis and complexation studies

M. Amélia Santos,* Estela Rodrigues and Margarida Gaspar

Centro de Química Estrutural, Complexo I, Instituto Superior Técnico,
Av. Rovisco Pais 1049-001 Lisboa, Portugal. E-mail: masantos@alfa.ist.utl.pt

Received 29th August 2000, Accepted 4th October 2000

First published as an Advance Article on the web 7th November 2000

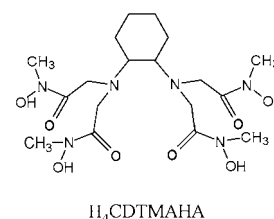
A new tetrahydroxamate ligand has been synthesized and its chelating properties studied, in aqueous solutions, with thorium(IV) and iron(III) as analogues of the actinides plutonium(IV) and (to some extent) americium(III). The architecture of this ligand is based on that of the cyclohexane-1,2-diyl-dinitrilotetraacetate complexone with hydroxamate instead of carboxylate groups. It has proven to form quite stable and water soluble complexes with these metal ions, up to pH 9. Besides the 1 : 1 (M : L) monomeric species formed under acidic conditions, the corresponding (2 : 2) dimeric complexes may also be admitted under physiological conditions. According to the magnetic properties and modelling calculations, the iron(III) dimer species should have some magnetic interaction between the metallic centres.

Introduction

For the treatment of human exposure to plutonium (Pu) and americium (Am) by inhalation, the administration of diethylenetriaminepentaacetic acid [carboxymethyliminobis-(ethylenetriolo)tetraacetic acid] (H_5DTPA) has been recommended for the treatment of radionuclide contamination.¹ However, it has also been pointed out that the H_5DTPA is not completely effective and it has been recognised that the synthetic analogues of siderophores (powerful chelating agents produced by micro-organisms to sequester the iron from the environment and deliver it into their cells) are both high specific and strong chelating agents for Pu^{4+} .²⁻⁴ Accordingly, a lot of research effort has recently been made on the complexation and solubilisation of plutonium⁵ and thorium⁶ by hydroxamate siderophores as well as on the design and synthesis of siderophore analogues (octadentate ligands), as actinide specific sequestering agents, mostly with four hydroxamate^{7,8} or hydroxypyridonate⁹⁻¹¹ chelating groups.

Although up to now our main research interest has been centred on the development of hydroxamate siderophore analogues and their interaction with Fe^{3+} ,¹²⁻¹⁴ the analogy between the chemistry of this metal ion and that of Pu^{4+} encourages us in the development of new sequestering agents for M^{4+} actinides, in particular, for potential *in vivo* clinical applications. Therefore, we report in this paper the design, synthesis and characterisation of a new tetrahydroxamate ligand, followed by equilibrium studies of its complexation with Fe^{III} and Th^{IV} , as analogues of plutonium(IV) [and of americium(III), to some extent] for safety reasons. Furthermore, the iron(III) complexation study deserves special attention because this ligand may be thought of as a potential siderophore analogue.

This new ligand, $H_4CDTMAHA$ (cyclohexane-1,2-diyl-dinitrilotetra(*N*-methylacetohydroxamic acid) is structurally similar to the complexone H_4CDTA (cyclohexane-1,2-diyl-dinitrilotetraacetic acid). It has four hydroxamate groups attached to a simple non-aromatic cyclic backbone (cyclohexane), to provide the octadenticity necessary for complete encapsulation of metal(IV) ions with M:L stoichiometry, as well as some pre-organisation of the chelating groups towards metal complexation. This ligand seems to have some advan-



tages over previous analogues, namely in terms of its potential usefulness as a drug. It does not include any aromatic groups (*cf.* refs. 8–11), its backbone skeleton has high commercial accessibility and, on the other hand, the *N*-substitution of the hydroxamate groups make it less susceptible to hydrolysis, as compared with previous compounds.⁷

Results

Design and synthesis

This hydroxamate CDTA derivative (CDTMAHA) may be regarded as a tetrapode on which four hydroxamate groups are placed on a single face of the molecule. The ligand was prepared in a relatively straightforward manner by two main steps starting from the commercially available tetracarboxylic acid H_4CDTA . This is condensed at room temperature with four *O*-benzyl-*N*-methylhydroxylamines, in the presence of a coupling agent, 1-[3-(dimethylamino)propyl]-1-ethylcarbodiimide (EDC), to give the tetra(*O*-benzylhydroxamic acid) derivative. *O*-Deprotection by catalytic hydrogenation (H_2 -Pd/C), as previously reported,¹² leads to the final product ($H_4CDTMAHA$).

Protonation

The acid–base properties of $H_4CDTMAHA$ were studied by potentiometry, aided by a ¹H NMR titration. This ligand has six protonation centres, two amine nitrogens and four hydroxamate groups. The protonation constants were obtained through fitting analysis of the potentiometric titration curve (Fig. 1). They are listed in Table 1, together with log *K* values of some structurally related compounds, such as H_4CDTA ¹⁵ and a tetrahydroxamate derivative, the *m*-xylenodiamino-*N,N'*-bis(propanohydroxamic) acid (H_4XDPHA).⁸ The values

Table 1 Stepwise protonation constants and global formation constants of the iron(III) and thorium(IV) complexes of H₄CDTMAHA and of relevant analogues

Ligand	H ⁺ log K _i	Fe ³⁺ log β _{Fe_pH_qL_r} ^a	Th ⁴⁺ log β _{Th_pH_qL_r} ^a
H ₄ CDTMAHA	9.91(3)	(1,4,1) 48.2(6)	(1,4,1) 46.37(3)
	8.88(3)	(1,3,1) 46.39(6)	(1,3,1) 41.99(6)
	8.52(4)	(2,3,2) 78.4(1)	(1,2,1) 36.23(9)
	7.80(4)		(1,1,1) 30.0(1)
	7.56(4)		
H ₄ CDTA ^b	6.42(7)		
	12.4	(1,0,1) 30.0	(1,1,1) 28.10
	6.15		(1,0,1) 25.6
	3.53		
H ₄ XDBHA ^c	2.42		
	10.18	(1,4,1) 47.43	(1,3,1) 45.92
	9.64	(1,3,1) 43.41	(1,2,1) 43.16
	8.99	(2,3,2) 74.16	(1,1,1) 39.65
	8.17		(1,0,1) 31.88
	6.38		
	5.36		

^a The (p,q,r) symbolism means a species with stoichiometry M_pH_qL_r.
^b Ref. 15. ^c Ref. 8.

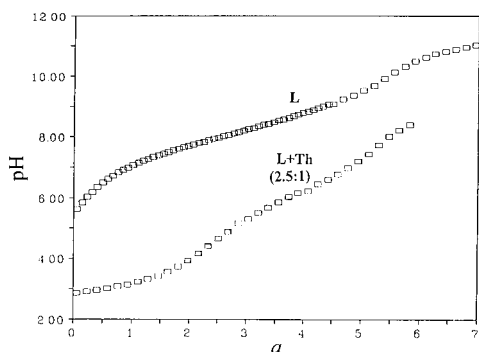


Fig. 1 Potentiometric titration curves (experimental points) for the ligand and the Th^{IV}-CDTMAHA system ($C_L/C_{Th} = 2.5/1$, $C_{Th} = 2.4 \times 10^{-3}$ M; $I = 0.1$ M (KNO₃); 25 °C); $a =$ moles of base added per mol of ligand present.

obtained [$\log K_1 = 9.91$, $\log K_2 = 8.88$, $\log K_3 = 8.52$, $\log K_4 = 7.80$, $\log K_5 = 7.56$, $\log K_6 = 6.42$] are according to expectations, namely in relation with the protonation constants of the amino groups in CDA (1,2-diaminocyclohexane; $\log K_1 = 9.71$, $\log K_2 = 6.59$)¹⁶ and those expected for the hydroxamate groups ($\log K = 8-10$).¹⁷ The proximity between these two ranges of values makes it difficult to attribute protonation constants to individual basic centres, thus suggesting there is some overlapping in these protonation processes. However, a considerable protonation shift is observed for the resonance peaks corresponding to the methylenic protons adjacent to the protonated amine groups [$\Delta\delta = 0.4-0.5$ ppm at pH around 10 and 6.5]. This indicates that $\log K_1$ and $\log K_6$ should mostly correspond to protonation of the amine groups, while the remaining values are mainly attributed to protonation of the hydroxamate groups.¹⁸ The most basic amine nitrogen atom is itself more basic in this ligand than in CDA. Probably, this is due to some stabilisation of the corresponding conjugated acid as a result of somewhat intramolecular hydrogen-bonding interaction between the ammonium protons and the γ -hydroxamate oxygen. Such an effect is expected to be lower in H₄CDTMAHA than in H₄CDTA because, in this case, the interaction involves a β -carboxylate oxygen.

Thorium complexation

Fig. 1 illustrates the potentiometric behaviour of the thorium(IV)-CDTMAHA complexation. There is a substantial depression of the titration curve of the ligand-metal ion binary

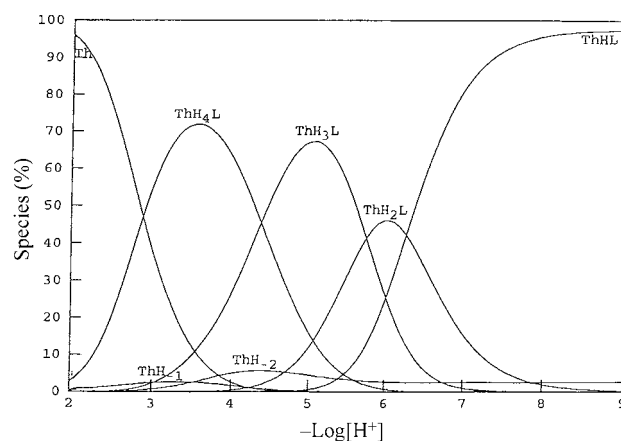


Fig. 2 Distribution diagram for the system Th^{IV}-CDTMAHA, as a function of pH. Conditions as in Fig. 1.

system, as compared to that of the ligand, thus indicating high affinity of the chelator for thorium(IV). In the studied range of pH (2–9) there was no precipitation, although above 8 the titration points take more time to stabilise. The best fitting model of experimental and calculated data corresponds to a set of four complexes: [Th(HL)]⁺, [Th(H₂L)]²⁺, [Th(H₃L)]³⁺ and [Th(H₄L)]⁴⁺. The global formation constants of the complexes are given in Table 1, together with literature data for corresponding complexes with the tetrahydroxamate XDPHA⁸ and CDTA.¹⁵ The calculated values for the formation constants are comparable (although slightly lower) to those of the tetrahydroxamate *m*-xylene derivative. Any difference can be attributed to differences in the protonation constants of the ligands, although some steric and/or electrostatic effects [between the positive charges of the protonated amine(s) and the metal ion] may contribute.

Analysis of the species distribution graph (Fig. 2) indicates that, at pH 3.5, the major complex species has four protons: two might be assigned to the amine basic sites and two to the hydroxamate sites. At neutral pH the major species [Th(HL)]⁺ has one amine group protonated and that proton can eventually interact with the other amine nitrogen (N–H···N). The existence of monocharged species for the ligand and the complex, under physiological conditions, is a factor in the good water solubility of both species. This is particularly important for the lipo-hydrophilic balance of ligand and complex, and deserved particular attention because of the potential utilisation of this new ligand as a drug. Noteworthy is the fact that the tris-hydroxamate desferrioxamine, which has been the elected drug for decorporation of aluminium(III) and iron(III) overload from patients,¹⁹ also has one protonated amine group at physiological pH.

In our equilibrium fitting model we have only included monomeric complexes with 1 : 1 stoichiometry (ThHL) because the ligand contains the four chelating moieties needed for a complete wrapping around of this 4+ metal ion. The corresponding dimeric species (Th₂H₂L₂) may be also admitted in this model, although these two species are indistinguishable by potentiometry. In fact, the dimeric structure is expected to be less sterically hindered than the monomeric one. In order to get an insight into the steric hindrance differences associated with each structure, we have performed a brief molecular simulation of both species by molecular mechanics methods, as a comparative study, using the CERIU²⁰ software package and the Universal force field.²¹ It was shown that the potential energy of the simulated monomer is higher than one half of the value obtained for the dimeric compound. The major contribution for the difference comes from non-bonded interactions (van der Waals contacts) because the monomeric complex structure gets quite crowded. Besides, from the minimum energy calculated structures (Fig. 3), it can be seen that the dimeric species has an

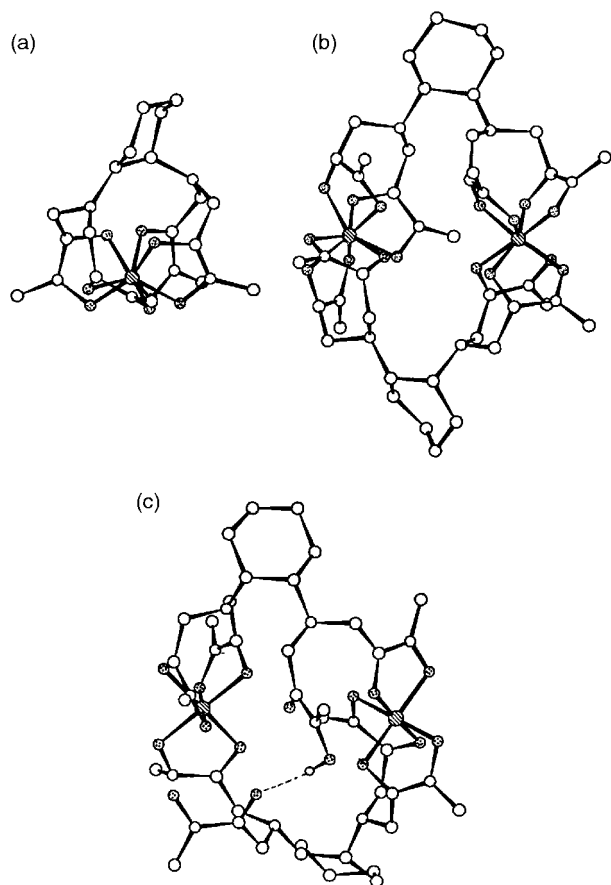


Fig. 3 Low-energy conformations calculated for Th(HL) (a), Th₂H₂L₂ (b) and Fe₂H₃L₂ (c) complexes. The metal ions are hatched, the oxygen atoms dotted; hydrogen atoms are omitted except for that involved in a hydrogen bond interaction.

eight-co-ordinate geometry which is much less distorted from the tetragonal antiprism (expected for a tetrakis-hydroxamate thorium(IV) complex)²² than the monomeric species.

Iron complexation

The stability constants for the iron(III) complexes were determined by Vis/UV spectrophotometry at 1:1 metal:ligand stoichiometry. Analysis of the set of spectra presented in Fig. 4 indicates complex formation below pH 2, thus suggesting a strong metal–ligand binding interaction. At pH 1.78 the CDTMAHA spectrum ($\lambda_{\text{max}} = 470 \text{ nm}$; $\epsilon = 1879 \text{ M}^{-1} \text{ cm}^{-1}$ per Fe) suggests a dihydroxamate co-ordination environment around the iron and corresponds to a red complex. In the range pH 4.5–9, λ_{max} is practically constant (440 nm), although there is an increase in the absorptivity up to pH 7 ($\epsilon = 3051 \text{ M}^{-1} \text{ cm}^{-1}$ per Fe) which became practically constant until pH 9. This behaviour is typical of the orange trishydroxamate iron(III) complexes which usually present a ligand to metal charge transfer transition with $425 < \lambda_{\text{max}} < 450 \text{ nm}$ and $2400 < \epsilon_{\text{max}}(\text{Fe}) < 3800 \text{ M}^{-1} \text{ cm}^{-1}$.²³ At higher pH there is a decrease in the absorbance and of λ_{max} due to probable formation of mixed hydroxo–hydroxamate complexes.

The equilibrium model obtained for the iron(III) complex includes two monomeric species Fe(H₄L)³⁺, Fe(H₃L)²⁺ and one dimeric species (Fe₂H₃L₂) whose global formation constants ($\log \beta$) are shown in Table 1. As suggested by the spectra, the first monomeric species should be assigned to the red complex with dihydroxamate co-ordination and four protonated groups (two hydroxamate and two amine). The release of one extra proton leads to the Fe(H₃L)²⁺ species with trishydroxamate co-ordination, having one hydroxamate and two amine groups protonated. Further deprotonation produces the dimeric species, also with a three-hydroxamate co-ordination. Each metallic

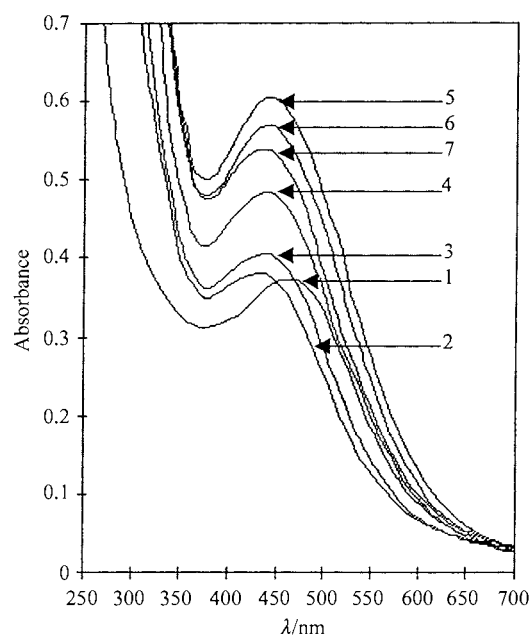


Fig. 4 Absorbance spectra of Fe^{III}–CDTMAHA as a function of pH: 1.78 (1), 4.52 (2), 5.52 (3), 6.00 (4), 8.50 (5), 10.02 (6) and 12.00 (7). $C_L/C_{\text{Fe}} = 10:1$, $C_{\text{Fe}} = 1.98 \times 10^{-4} \text{ M}$; $I = 0.1 \text{ M}$ (KNO₃); 25.0 °C.

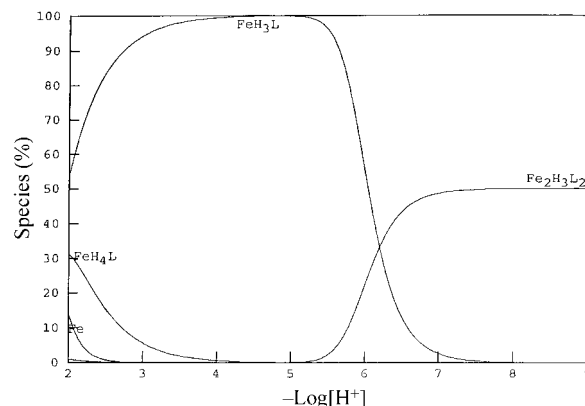


Fig. 5 Distribution species for the system Fe^{III}–CDTMAHA as a function of pH. Conditions as in Fig. 4.

centre may use two hydroxamate groups are from one ligand and one hydroxamate group from the other. In this dimeric species each ligand should have one protonated amine, which may be hydrogen bonded with the other amine. Furthermore, according to the proposed equilibrium model, only one hydroxamate group is protonated. Probably, it has a hydrogen bond like interaction with the corresponding non-protonated and non-co-ordinated hydroxamate oxygen atom of the other ligand.

Fig. 5 shows the species distribution diagram, under the conditions used in the spectrophotometric titration ($C_L/C_{\text{Fe}} = 10$, $C_{\text{Fe}} = 1.98 \times 10^{-4} \text{ M}$). It is suggested that between pH 4 and 5.3 there is complete formation of the Fe(H₃L) species and, for higher pH, that the monomeric species changes into the dimeric species which is completely formed from pH 7.

The magnetic properties, namely the solution magnetic moment (μ), were measured in D₂O solution by the Evans method, without correction of the solvent effect and diamagnetic contribution.^{24,25} In the pH range (7–9) attributed to formation of the dimeric species, the calculated values for μ (5.52–5.38 μ_B) are consistent with the existence of a binuclear species with antiferromagnetic coupling. The values are close to that obtained for another dimeric Fe₂L₃ dihydroxamate complex (5.5 μ_B) studied in our research group.²⁶ Moreover, a value of 5.4 μ_B was found for an iron bis- μ -oxo-dimer.²⁷

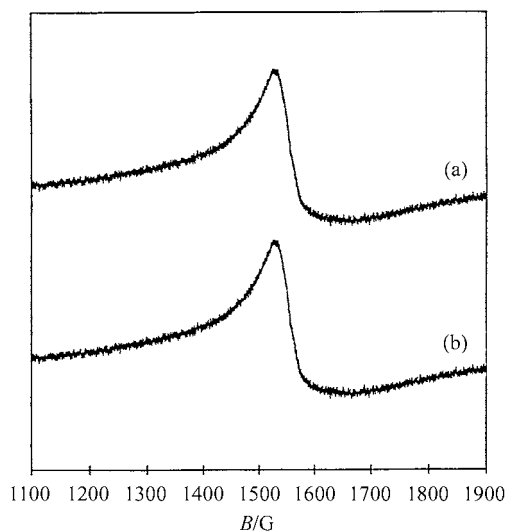


Fig. 6 EPR spectra of (a) CDTMAHA and (b) PIPDMAHA iron(III) complexes (Fe_2L_3) in frozen D_2O solutions ($C_L/C_{\text{Fe}} = 3:2$; $\text{pD}^* = 7$, $C_{\text{Fe}} = 1.0 \times 10^{-3}$ M, 100 K; frequency 9.34 GHz and modulation frequency 100 kHz).

The electron paramagnetic resonance (EPR) results also suggest the existence of a dimeric diiron(III) complex. At pH 7.0 the spectrum presents a peak at $g = 4.3$, typical of high spin octahedral iron(III) (see Fig. 6). The band linewidth (135 G) is indicative of dipole–dipole interaction, thus giving support to the dimeric structure, as previously found for other dimeric hydroxamate complexes, such as that with piperazine-1,4-bis(*N*-methylacetohydroxamic acid), $\text{H}_2\text{PIPDMAHA}$.^{26,28}

The structure of the dimer $\text{Fe}_2\text{H}_3\text{L}_2$ simulated by molecular mechanics (Fig. 3c) has each metal co-ordinated in a octahedral environment provided by three hydroxamate moieties. The calculated distance between the iron(III) centres (6.41 Å) also gives support to the existence of the above dimeric species with magnetic interaction between the metal centres.²⁹

Redox properties of the Fe^{III} –CDTMAHA system were studied by cyclic voltammetry, in particular at physiological pH, due to their importance for *in vivo* iron transport, as a potential siderophore analogue. The redox potential value (–586 V vs. the standard calomel electrode, SCE) is in the range of the physiological reductors and comparable to that (–588 V) of rhodotorulic acid, a naturally occurring siderophore.²⁷ The set of electrochemical results suggested an EC global mechanism which includes a quasi-reversible electrochemical process (E) followed by a chemical irreversible reaction (C).³⁰ Evaluation of the stability constant for the iron(III) complex was not carried out for this system since it was impossible to find any situation with complete reversibility for the electrochemical reaction (either due to the coupled chemical reaction, for lower scan rates, or due to adsorption processes, for higher scan rates).

The Fe^{III} –CDTMAHA complexes showed biological activity towards the bacteria *Morganella morganii* and *Proteus mirabilis*.¹³

Experimental

Instrumentation

The ^1H NMR spectra were recorded on a Varian Unity 300 spectrometer at 25 °C. Chemical shifts are reported in ppm (δ) from internal references such as tetramethylsilane (TMS) in organic solvents and sodium 3-(trimethylsilyl)[2,2,3,3,3- $^2\text{H}_5$]-propionate in D_2O . The following abbreviations are used: s = singlet; d = doublet; t = triplet; m = multiplet; bs = broad singlet; bd = broad doublet; bt = broad triplet. The EPR spectra were obtained by using a Bruker ESP ER 200D spectrometer

(X-band) in frozen D_2O solutions with 20% ethylene glycol to give a good glass ($C_L/C_{\text{Fe}} = 3:2$; $C_{\text{Fe}} = 1.0 \times 10^{-3}$ M; $\text{pD}^* = 7.0$; $T = 100$ K; modulation frequency 100 kHz). The magnetic moment of the iron(III) complexes in aqueous solutions ($C_M = 2 \times 10^{-3}$ M; $C_L = 1 \times 10^{-2}$ M) was measured in an NMR tube (Wilmad Glass Co, Inc. WGS-5BL) following the method of Evans with neglect of (i) the solvent correction for diluted solutions and small molecules^{24,25} and (ii) the correction for diamagnetic contributions.^{25b} Infrared (IR) spectra were recorded on a Perkin-Elmer 683 spectrophotometer. Melting temperatures were measured with a Leica Gallen III hot-stage apparatus and are uncorrected. Elemental analysis was performed on a Fisons EA1108 CHN/O instrument. Mass spectra were obtained in a VG TRIO-2000 spectrometer; FAB spectra were recorded with the samples dispersed in a matrix of thioglycerol or 3-nitrobenzyl alcohol.

Potentiometric titrations

Potentiometric measurements were carried out using a Crison Digital 517 instrument with an Ingold U1330 glass electrode and an Orion 90-00.11 Ag–AgCl reference electrode. The electrode calibration was carried out daily from a titration of a strong acid (HNO_3 , 0.1 M) with a strong base (KOH, 0.1 M). In all potentiometric titrations the equilibrium measurements were conducted at 25.0 ± 0.1 °C and at a constant ionic strength $I = 0.1$ M (KNO_3). The ligand was weighed directly into the potentiometric cell and the exact concentrations of the ligand were confirmed by Gran's method.³¹ The Th^{IV} was added to the ligand–electrolyte solution from a stock solution of $\text{Th}(\text{NO}_3)_4$, 5.0×10^{-2} M. The potentiometric data were analysed with the SUPERQUAD program³² and the species distribution diagrams were obtained with the SPEA program.³³ Equilibrium chemical models were selected on the basis of a critical evaluation of the least-squares results and of the statistical analysis of the weighted residuals, namely the statistical parameters ($\chi^2 < 12.6$ and $\sigma \leq 1$).³⁴

Spectrophotometric measurements

Solutions of Fe^{III} –CDTMAHA complexes were generated *in situ* by addition, to an excess of the ligand, of a standard metal ion solution containing 1000 ppm $\text{Fe}(\text{NO}_3)_3$ in HNO_3 (0.5 M). All solutions were thermostatted at 25.0 ± 0.1 °C and the supporting electrolyte was KNO_3 , 0.1 M. The pH measurements were done using a 420 A Orion pH-meter, equipped with an Orion 91-03 glass calomel combined electrode. All spectra were measured on a Lambda 9 Perkin-Elmer spectrophotometer. The stability constants for the iron(III) complexes were evaluated from the spectrophotometric titration data, using the PSEQUAD computer program,³⁵ taking into account the calculated fitting parameter ($f < 1 \times 10^{-2}$).

Syntheses

Cyclohexane-1,2-diylidinitrilotetra(*O*-benzyl-*N*-methylacetohydroxamate) 1. 3,3-Dimethylaminopropyl-1-ethylcarbodiimide (1.099 g, 5.8 mmol) was added to a solution of cyclohexane-1,2-diylidinitrilotetraacetic acid (0.261 g, 0.72 mmol) and *O*-benzyl-*N*-methylhydroxylamine (0.752 g, 4.3 mmol) in THF–water (2:1, 100 mL). The mixture was stirred at room temperature for 6 h, with pH 4.8 adjustment. The end of the reaction was detected by TLC. The reaction mixture was neutralized and extracted with ethyl acetate, and the organic extract was washed with a saturated solution of NaCl and dried with Na_2SO_4 . Purification of the product by flash chromatography yielded 0.198 g of compound **1**, as a pale white powder (34% yield), mp 102–104 °C IR (KBr): 1570 cm^{-1} (C=O). ^1H NMR (D_2O –DSS): δ 1.49, 1.63 (2 × bq, 4H, $\text{C}^4\text{HHC}^5\text{HH}$, $\text{C}^4\text{HHC}^5\text{HH}$), 2.59, 2.79 (2 × bq, 4H, C^3HH to C^6HH , C^3HH

to C⁶HH), 2.97 (m, 2H, NCH), 3.13 (s, 12H, CH₃), 3.19 (s, 8H, NCH₂CO), 4.76 (bs, 8H, C₆H₁₀CH₂) and 7.29 (m, 20H, C₆H₁₀H). FAB-MS (*m/z*): 823, (M + 1)⁺.

Cyclohexane-1,2-diyl dinitrilotetra(*N*-methylacetohydroxamic acid) 2 (H₄CDTMAHA). Palladium on carbon (5%, 0.16 g) was added to a solution of compound **1** in methanol (25 mL). The reaction was stirred under H₂ (1 atm) at room temperature for 5 h. The catalyst was filtered off, and the solvent removed *in vacuo* to provide **2** as a pale white solid. Recrystallisation from methanol–diethyl ether gave white crystals (0.098 g, 96%), mp 156–158 °C. IR (KBr): 1640 cm⁻¹ (C=O). FAB-MS (*m/z*): 463, (M + 1)⁺. ¹H NMR (D₂O–DSS): δ 1.13, 1.23 (2 × bt, 4H, C⁴HHC⁵HH, C⁴HHC⁵HH), 1.79, 2.15 (2 × bt, 4H, C³HH to C⁶HH, C³HH to C⁶HH), 3.21 (s, 12H, CH₃), 3.33 (m, 2H, NCH), 3.70, 3.94 (2 × bs, 8H, NCHH). Calc. for C₁₈H₃₄N₆O₈·3.5H₂O: C, 41.14; H, 7.86; N, 15.99. Found: C, 41.32; H, 7.83; N, 16.04%.

Acknowledgements

The authors are grateful to Fundação para a Ciência e Tecnologia (FCT) (project PRAXIS/PCEX/QUI/85/96) and the COST D8/0010 program for financial support and also to Professor J. Paulo Telo for kindly providing the EPR spectra.

References

- 1 G. N. Stradling, *J. Alloys Comp.*, 1998, **271–273**, 72; M. H. Bhatta Charyya, B. D. Breitenstein, H. Métivier, B. A. Muggenburg, G. N. Stradling and V. Volf, *Radiat. Prot. Dosim.*, 1992, 41.
- 2 K. N. Raymond, G. Muller and B. F. Matzanke, *Top. Curr. Chem.*, 1994, **123**, 49.
- 3 P. W. Durkin, N. Jeung, S. J. Rodgers, P. N. Turowski, F. L. Weite and D. L. White, *Radiat. Prot. Dosim.*, 1989, **26**, 351.
- 4 G. N. Stradling, *Radiat. Prot. Dosim.*, 1994, **53**, 297.
- 5 M. P. New, J. H. Matonic, C. E. Ruggiero and B. L. Scott, *Angew. Chem., Int. Ed.*, 2000, **39**, 1442.
- 6 M. Bouby, I. Billard and J. MacCordick, *J. Alloys Comp.*, 1998, **271–273**, 206.
- 7 N. Koshti, V. Huber, P. Smith and A. S. Gopalan, *Tetrahedron*, 1994, **50**, 2657.
- 8 A. S. Gopalan, V. J. Huber, O. Zincircioglu and P. H. Smith, *J. Chem. Soc., Chem. Commun.*, 1992, 1266.
- 9 L. Dasaradhi, P. C. Stark, V. J. Huber, P. H. Smith, G. D. Jarvinen and A. S. Gopalan, *J. Chem. Soc., Perkin Trans. 2*, 1997, 1187.

- 10 T. N. Lambert, L. Dasaradhi, V. J. Huber and A. S. Gopalan, *J. Org. Chem.*, 1999, **64**, 6097.
- 11 J. Xu, B. Kullgren, P. W. Durbin and K. N. Raymond, *J. Med. Chem.*, 1995, **38**, 2606.
- 12 M. A. Esteves, M. C. T. Vaz, M. L. S. Simões Gonçalves, E. Farkas and M. A. Santos, *J. Chem. Soc., Dalton Trans.*, 1995, 2565.
- 13 M. Gaspar, M. A. Santos, K. Krauten and G. Winkelmann, *Biometals*, 1999, **12**, 209.
- 14 M. Gaspar, R. Grazina, A. Bodor, E. Farkas and M. A. Santos, *J. Chem. Soc., Dalton Trans.*, 1999, 799.
- 15 A. E. Martell and R. M. Smith, *Critical Stability Constants*, Plenum Press, New York, 1974, vol. 1, pp. 236–240.
- 16 A. E. Martell and R. M. Smith, *Critical Stability Constants*, Plenum Press, New York, 1974, vol. 2, p. 46.
- 17 G. Anderegg, F. L'Éplattenier and G. Schwarzenbach, *Helv. Chim. Acta*, 1963, **156**, 1400.
- 18 M. A. Santos, M. A. Esteves, M. C. Vaz, J. J. R. Fraústo da Silva, B. Noszal and E. Farkas, *J. Chem. Soc., Perkin Trans. 2*, 1997, 1977.
- 19 R. A. Yokel, *J. Toxicol. Environ. Health*, 1994, **41**, 131.
- 20 CERIU² Program, Version 3. 4, Molecular Simulation Inc, Cambridge, 1998.
- 21 A. K. Rappe, C. J. Casewit, K. S. Colwell, W. A. Goddard and W. M. Skiff, *J. Am. Chem. Soc.*, 1992, **114**, 10024.
- 22 W. L. Smith and K. N. Raymond, *J. Am. Chem. Soc.*, 1981, **103**, 3341.
- 23 S. Blanc, P. Yakinevitch, E. Leize, M. Meyer, J. Libman, A. V. Dorsselaer, A.-M. Albrecht-Gary and A. Shanzer, *J. Am. Chem. Soc.*, 1997, **119**, 4939.
- 24 D. F. Evans, *J. Chem. Soc.*, 1959, 2003.
- 25 (a) D. H. Grant, *J. Chem. Educ.*, 1995, **72**, 39; (b) C. Piguet, *J. Chem. Educ.*, 1997, **74**, 815.
- 26 M. A. Santos, M. A. Esteves, M. C. Vaz and M. L. S. Simões Gonçalves, *J. Chem. Soc., Dalton Trans.*, 1993, 927.
- 27 Z. Hou, K. N. Raymond, B. O'Sullivan and T. W. Esker, *Inorg. Chem.*, 1998, **37**, 6630.
- 28 M. A. Santos, M. Gaspar, M. L. S. Gonçalves and M. T. Amorim, *Inorg. Chim. Acta*, 1998, **278**, 51.
- 29 C. J. Carrano, S. R. Cooper and K. N. Raymond, *J. Am. Chem. Soc.*, 1979, **101**, 599.
- 30 R. S. Nicholson and I. Shain, *Anal. Chem.*, 1964, **36**, 706.
- 31 G. Gran, *Analyst (London)*, 1952, **77**, 661.
- 32 P. Gans, A. Sabatini and A. Vacca, *J. Chem. Soc., Dalton Trans.*, 1985, 1195.
- 33 A. E. Martell and R. J. Motekaitis, *Determination and Use of Stability Constants*, VCH, New York, 1988.
- 34 A. Sabatini, A. Vacca and P. Gans, *Talanta*, 1974, **21**, 53.
- 35 L. Zékány and I. Nagypál, in *Computational Methods for the Determination of Stability Constants*, ed. D. Legget, Plenum, New York, 1985.